

Visceral obesity stimulates anaphase bridge formation and spindle assembly checkpoint dysregulation in radioresistant oesophageal adenocarcinoma

A. M. Mongan¹ · N. Lynam-Lennon¹ · R. Casey¹ · S. Maher² ·
G. Pidgeon¹ · J. V. Reynolds¹ · J. O'Sullivan¹

Received: 17 April 2015 / Accepted: 14 September 2015 / Published online: 16 October 2015
© Federación de Sociedades Españolas de Oncología (FESEO) 2015

Abstract

Purpose Oesophageal adenocarcinoma is an exemplar model of obesity-associated cancer. Locally advanced disease is treated with neoadjuvant chemoradiotherapy, and survival rates are highest in patients demonstrating a pathological response following neoadjuvant therapy. Given that 55 % of oesophageal adenocarcinoma patients are obese, uncovering the effect of adipose tissue on radioresponse is clinically relevant. This study investigates if adipose tissue activates genomic instability events in radioresponsive (OE33P) and radioresistant (OE33R) oesophageal cancer cell lines and tumour samples.

Methods OE33R and OE33P were cultured with adipose-conditioned media derived from oesophageal adenocarcinoma patients ($n = 10$). Anaphase bridges, a marker of genomic instability, were enumerated in both cell lines following treatment with adipose media, and normalised to cell number. Genomic instability is regulated by the spindle assembly complex. Expression of two spindle assembly complex genes (MAD2L2, BUB1B) was assessed using qPCR, and validated in patient tumour specimens from visceraally obese ($n = 46$) and nonobese patients ($n = 41$). **Results** Adipose-conditioned media increased anaphase bridging in OE33R ($p < 0.0001$), with a threefold increase

in OE33R compared to OE33P ($p < 0.01$). Levels of anaphase bridges in OE33R cells correlated with visceral obesity status as measured by waist circumference ($R = 0.709$, $p = 0.03$) and visceral fat area ($R = 0.794$, $p = 0.006$). Adipose tissue altered expression of MAD2L2 in vitro. In vivo, MAD2L2 expression was higher in visceraally obese oesophageal adenocarcinoma patients compared with nonobese patients ($p < 0.05$).

Conclusions Anaphase bridge levels are influenced by obesity and radiosensitivity status in oesophageal adenocarcinoma. Furthermore, visceral adipose-conditioned media stimulates dysregulation of the spindle assembly complex in oesophageal adenocarcinoma patients.

Keywords Oesophageal cancer · Obesity · Genomic instability · Radiotherapy

Introduction

The incidence of oesophageal adenocarcinoma is increasing more than any other cancer in the western world, paralleling the current epidemic of obesity [1]. In fact, oesophageal adenocarcinoma is the strongest model of a cancer associated with obesity, making it the ideal model for studying the molecular effects of obesity [2]. Visceral adipose tissue secretes factors in a paracrine and systemic manner, which facilitates tumour development by promoting the acquisition of the hallmarks of cancer [1]. One of the emerging enabling hallmarks of cancer is genomic instability, an established feature of most forms of cancer and pre-malignant conditions such as Barrett's oesophagus, as well as being associated with obesity [3, 4]. Genomic instability refers to the increased tendency of the genome to acquire mutations when the processes involved in maintaining and replicating the

✉ J. O'Sullivan
osullij4@tcd.ie

¹ Department of Surgery, Trinity Centre for Health Sciences, St. James's Hospital, Dublin 8, Ireland

² Cancer Biology & Therapeutics Lab, School of Biological, Biomedical & Environmental Sciences, University of Hull, Cottingham road, Hull HU6 76X, UK

genome are dysfunctional [3]. We and others have demonstrated that anaphase bridges are closely related to genomic instability in human disease [5, 6]. Anaphase bridges consist of DNA strands connecting the nuclei of daughter cells which fail to resolve following anaphase in cell division [7]. The majority of anaphase bridges formed will break, giving rise to structural chromosomal rearrangement, with a net gain of chromosomal material in one daughter cell, and a corresponding net loss in the other daughter cell [7]. Activation of the spindle assembly checkpoint is also essential in the prevention of genomic instability [8]. Checkpoint deficiencies enable chromosomal rearrangements to be duplicated, leading to genomic amplifications and deletions, generating a pro-cancer genome [8].

Accumulation of genomic instability events (including anaphase bridge formation and spindle assembly checkpoint dysregulation), is associated with poor prognosis across a range of cancer types, and with resistance to therapy [9, 10]. Obesity may be implicated in the initiation of genomic instability events [11]. Obesity is associated with poor survival in a range of cancers including oesophageal, and studies have demonstrated that visceral obesity is an independent predictor of outcome after anti-angiogenic treatment in colorectal and renal cell carcinoma [2, 12, 13]. The interaction between obesity and treatment response in oesophageal adenocarcinoma has not been adequately addressed. Neoadjuvant chemoradiotherapy improves the overall survival of patients with advanced adenocarcinoma of the oesophagus according to current Cochrane analysis [14], meta-analysis [15], and the CROSS-trial [16]. Given that 55 % of oesophageal adenocarcinoma patients are obese, the question of whether obesity is associated with treatment failure following radiation therapy is clinically relevant [17]. The aim of this study was to assess if visceral adipose tissue drives genomic instability events, and identify if these instability events are associated with a radioresistant phenotype in oesophageal adenocarcinoma.

Materials and methods

Oesophageal adenocarcinoma radioresistant cell line OE33R and passage matched control OE33P

The human oesophageal adenocarcinoma OE33 cell line was purchased from the American Collection of Cell Cultures (ATCC, Virginia, USA). The radioresistant cell line OE33R was established as previously described [18]. Briefly, the OE33 cell line was exposed to clinically relevant fractionated doses of radiation to create an isogenic radioresistant subline called OE33R. Parental cells were mock-irradiated. Both OE33R and its age and passage matched parental counterpart, OE33P, were cultured as

monolayers in Roswell Park Memorial Institute (RPMI-1640) medium supplemented with 10 % foetal calf serum and 1 % penicillin–streptomycin and maintained at 37 °C in 95 % humidified air containing 5 % CO₂.

Patient recruitment and anthropometry

Ethical approval was granted from the St. James's Hospital and AMNCH (Adelaide and Meath hospital incorporating the National Children's Hospital) Ethics review board. All oesophageal adenocarcinoma patients undergoing elective surgical resections were invited to participate. Patients gave informed consent for sample collection for research. Body weight, height, visceral fat area and waist circumference were measured and body mass index (BMI) calculated for all patients. Computed tomography (CT) measurement of visceral fat area is the gold standard marker of obesity, and was used as the primary indicator of obesity status in this study [1]. Visceral fat area was calculated by a radiologist using a previously standardised and validated technique, and visceral fat areas in excess of 130 m² were classified as obese [19]. All oesophageal adenocarcinoma tumour samples were assessed as per standard guidelines and histologically confirmed as oesophageal adenocarcinomas by a pathologist [20].

Adipose tissue processing

Visceral adipose tissue was excised at the beginning of the surgical resection, and processed according to an adapted protocol from Fried and Moustaid-Moussa [17, 21]. Adipose-conditioned media (ACM) was prepared as follows: a 5-g sample of minced and washed adipose tissue was incubated in 10 mL of serum-free M199 media supplemented with 50 µg/mL gentamicin (Biosciences; Dublin, Ireland), for 72 h at 37 °C and 5 % CO₂, and the sample filtered to remove adipose tissue fragments.

Co-culture with adipose-conditioned media

Cells were seeded in 12-well plates at a concentration of 2×10^4 cells/well for anaphase bridge enumeration and 6×10^4 cells/well for spindle assembly checkpoint gene expression and allowed to adhere. 0.5 mL of the adipose-conditioned media or M199 control media was added to the wells and the plates incubated for 24 and 72 h.

Anaphase bridge enumeration

Cells were fixed with 3.7 % paraformaldehyde, stained with haematoxylin, and washed in 50, 70 and 100 % ethanol before drying on the bench for 1 h. Anaphase bridges were defined as one or more interconnected strands between

daughter nuclei, cells with no interconnecting strands were scored as negative. Numbers of anaphase bridges were counted using an Olympus CKX41 (Tokyo, Japan) microscope with objective power of 100× objective and eyepiece power of 20×. Crystal violet assays were performed at the same time as anaphase bridge level enumeration to determine fold change in cell number in OE33P and OE33R cells following treatment with adipose-conditioned media, to allow for normalisation to change in cell number. Cells were seeded in triplicate in 96-well plates at a concentration of 5000 cells/well and allowed to adhere overnight prior to coculture with 50 µL adipose-conditioned media or M199 control media for 24 and 72 h at 37 °C. Following 24 and 72 h, the media was decanted. Cells were washed with PBS and fixed with 1 % glutaraldehyde at room temperature for 15 min. Cells were washed with PBS and stained with 500 µL 0.1 % crystal violet at room temperature for 30 min. Crystal violet was discarded and the plate washed gently with tap water, then left to air dry upside down for 10 min. Cells were resuspended in 400 µL Triton X solution and incubated on a shaker for 15 min at room temperature. 100 µL of sample was transferred into a 96-well plate. The absorbance was read at 590 nm in a VERSAMax microplate reader (Molecular devices, CA, USA). In this study, levels of anaphase bridges are expressed as fold change in anaphase bridge numbers normalised to change in cell number in cells.

Real-time PCR

RNA was harvested from OE33R and OE33P cell lines using the TriReagent protocol. For tissue samples, oesophageal adenocarcinoma tumour specimens were excised from patients following recruitment to the upper gastrointestinal biobank. RNA was extracted using Qiagen Rneasy Mini kit (Qiagen Inc., CA, USA), and quantified using a Nanodrop 1000 spectrophotometer v3.3 (Thermo Scientific). cDNA was synthesised by adding random primers (0.5 µg/µL) to 500 ng RNA, heating the sample to 70 °C for 10 min in order to denature the RNA, and immediately chilling on ice for at least 1 min. A master mix was added to each sample, containing: RNaseOUT recombinant ribonuclease inhibitor (1 unit/µL), dNTPs (10 mM, prepared as a 1:1:1:1 ratio of dATP, dGTP, dTTP and dCTP), Bioscript reverse transcriptase (200 units/µL) in 5× Bioscript reaction buffer. This mixture was then incubated at 37 °C for 3 h and 70 °C for 10 min. 1 µL of the resulting cDNA template was used to investigate gene expression. The reverse transcriptase enzyme and buffer were purchased from Bioline (Bioline, Kilkenny, Ireland), all other reagents were purchased from Invitrogen (Invitrogen Corp., CA, USA). qPCR was performed in the oesophageal adenocarcinoma cell lines and tumour samples, to quantify mRNA expression of spindle assembly checkpoint genes relative to the endogenous

control. This was performed using a TaqMan® assay kit (Applied Biosystems), and 18S was the endogenous control (18S ribosomal RNA) used for data normalisation. Probe sets were FAM labelled: 18s Assay ID: Hs 99999901_s1: MAD2L2 Assay ID: Hs01057448_m1: BUB1b Assay ID: Hs01084828_m1. Analysis was performed using SDS 2.3 and SDS RQ 1.2 relative quantification software (Applied Biosystems). Gene expression in cell lines was expressed as fold increase in expression relative to control. Gene expression in patient tumour samples was expressed as relative quantification (RQ) values. One sample was set as the calibrator for the analysis.

Statistical analysis

Statistical analysis was performed using Graphpad Prism 5 software. All data are expressed as mean ± standard error of the mean (SEM). When two groups were compared a two-tailed Student's *t* test was used. Correlation between obesity status and genomic instability events was assessed using Pearson's correlation. Comparison of patient cohorts was performed using the Mann–Whitney *U* test. For all analysis, $p \leq 0.05$ was considered to be statistically significant.

Results

Adipose-conditioned media stimulates anaphase bridge formation

Figure 1a shows a representative image of an anaphase bridge. Adipose-conditioned media used in anaphase bridge enumeration and spindle assembly checkpoint gene expression studies was derived from oesophageal adenocarcinoma patients. Anthropometric data for these patients are summarised in Table 1 (supplementary data). OE33P cells treated with adipose-conditioned media for 24 h showed a twofold increase in anaphase bridge formation compared to OE33P cells exposed to control media only ($p < 0.01$). OE33P cells treated with adipose-conditioned media for 72 h demonstrated significantly lower levels of bridge formation compared to untreated cells (twofold decrease, $p < 0.0001$) (Fig. 1b). Higher levels of anaphase bridge formation were detected at 24 compared to 72 h ($p < 0.05$). There was no difference in levels of bridging induced by adipose-conditioned media from nonobese compared to obese patients ($n = 5$ obese, 5 nonobese, data not shown).

OE33R cells exposed to adipose-conditioned media for 24 h showed a sixfold increase in anaphase bridge formation compared to controls ($p < 0.0001$). OE33R cells exposed to adipose-conditioned media for 72 h demonstrated a twofold increase in levels of anaphase bridge formation compared to controls ($p < 0.01$) (Fig. 1b). This

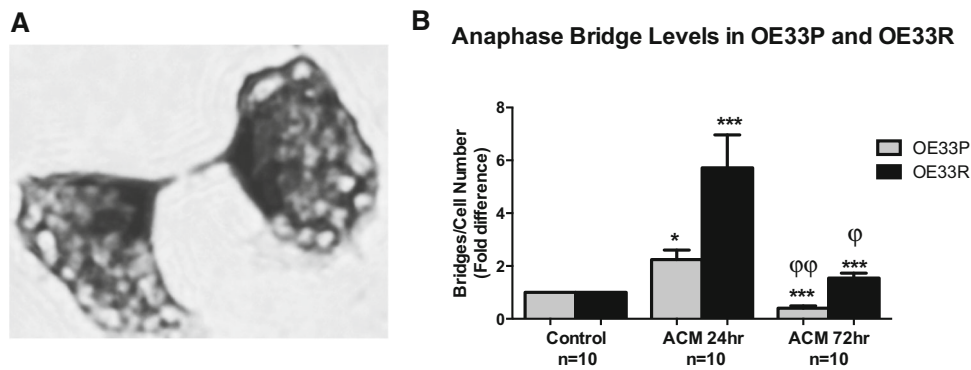


Fig. 1 Levels of anaphase bridging are enumerated in OE33P and OE33R cell lines following exposure to adipose-conditioned media (ACM) for 24 and 72 h. **a** Representative image of anaphase bridges enumerated in this study. **b** Increased bridging is seen in OE33P following exposure to ACM compared to control media for 24 h ($p < 0.05$), but decreased bridging is seen in OE33P following treatment with ACM for 72 h. Increased bridging is seen in OE33R following exposure to ACM for 24 and 72 h. Levels of bridging induced by ACM are higher in OE33R compared to OE33P at both 24

and 72 h. Data are expressed as fold increase in bridging per fold increase in cell number in $n = 10$ patients, results represent the average from three independent experiments. Analysis was performed using paired Student's t test to compare ACM-treated OE33P and OE33R versus controls, $*p < 0.05$, $**p < 0.001$, $***p < 0.0001$; an unpaired two-tailed Student's t test was used to compare ACM-treated OE33P cells versus ACM-treated OE33R cells, $^{\phi\phi}p < 0.05$, $^{\phi\phi\phi}p < 0.001$, $^{\phi\phi\phi\phi}p < 0.0001$. ACM adipose-conditioned media

Table 1 Anthropometric data for patient adipose-conditioned media used in anaphase bridge enumeration and spindle assembly checkpoint gene expression studies

Patient	Age	Gender	Body mass index (kg/m ²)	Waist circumference (cm)	Visceral fat area (cm ²)
1	68	Male	25	95	127.5
2	58	Male			83.0
3	50	Male	23.2	94	87.6
4	46	Male		100.3	17.0
5	58	Male	20.6	80	30.8
6	68	Male	28.8	104	284.8
7	72	Male	30.1	106.7	240.6
8	67	Male	27.2	102	216.8
9	62	Male	33.8	126	383.8
10	71	Male	22.9	88	227.0

increase was significantly higher in cells treated with adipose-conditioned media from obese compared to nonobese patients ($p < 0.01$, $n = 5$ obese 5 nonobese, data not shown). Higher levels of anaphase bridge formation were seen at 24 compared to 72 h ($p < 0.05$). Levels of anaphase bridging were significantly higher in adipose-conditioned media-treated OE33R compared to OE33P cells at both 24 ($p < 0.01$) and 72 h ($p < 0.0001$) (Fig. 1b). There was no difference in levels of anaphase bridge formation between untreated OE33P and OE33R cell lines (data not shown).

Anaphase bridge formation in adipose-conditioned media-treated cells correlates with obesity status

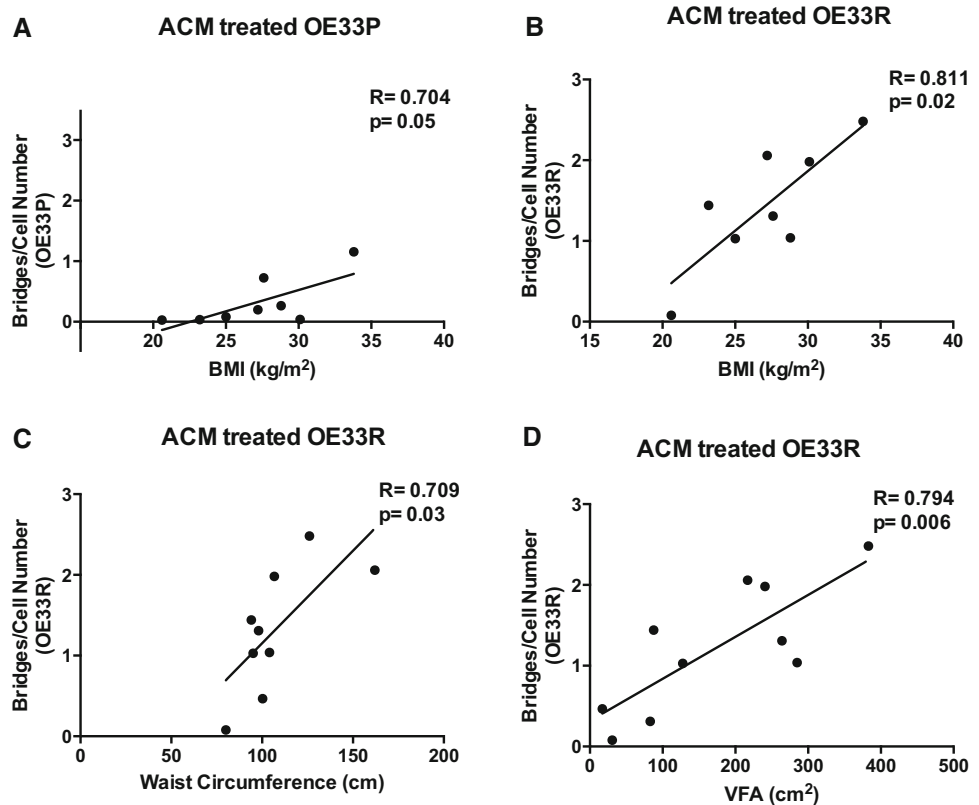
Levels of anaphase bridge formation in the OE33P cell line at 72 h, correlated with obesity status as measured by BMI ($R = 0.704$, $p = 0.05$) (Fig. 2a), but did not correlate with

waist circumference or visceral fat area (data not shown). Anaphase bridge formation in OE33R cells at 72 h correlated with obesity as measured by BMI ($R = 0.811$, $p = 0.02$), waist circumference ($R = 0.709$, $p = 0.03$) and visceral fat area ($R = 0.794$, $p = 0.006$) (Fig. 2b–d). Levels of anaphase bridge formation in OE33P and OE33R following 24 h of adipose-conditioned media treatment did not correlate with obesity status (data not shown).

Adipose-conditioned media drives MAD2L2 expression in OE33P and OE33R

There was a sixfold increase in MAD2L2 expression in OE33P cells following adipose-conditioned media treatment for 24 h ($p < 0.0001$). A twofold increase in expression was detected following adipose-conditioned media treatment for 72 h ($p < 0.01$) (Fig. 3a). Significantly higher expression was seen following exposure to adipose-

Fig. 2 Levels of anaphase bridge formation in OE33P and OE33R following 72-h treatment with ACM correlate with obesity status. **a** Anaphase bridge formation in OE33P correlates with BMI ($R = 0.704$, $p = 0.05$), but did not correlate with waist circumference or visceral fat area (data not shown). Anaphase bridge formation in OE33R correlates with **b** BMI ($R = 0.811$, $p = 0.02$), **c** waist circumference ($R = 0.709$, $p = 0.03$), and **d** visceral fat area (VFA) ($R = 0.794$, $p = 0.006$). Analysis was performed using Pearson correlation coefficient. ACM adipose-conditioned media, BMI body mass index, VFA visceral fat area, R Pearson's correlation coefficient



conditioned media from obese compared to nonobese patients for 72 but not 24 h ($p < 0.05$, $n = 5$ nonobese, $n = 5$ obese, data not shown). MAD2L2 expression was markedly increased in OE33R following adipose-conditioned media treatment for 24 h (tenfold increase, $p < 0.01$), but was unchanged following 72 h of adipose-conditioned media treatment (Fig. 3a). There was no difference in MAD2L2 expression in OE33R following treatment with adipose-conditioned media from nonobese compared to obese patients (data not shown). MAD2L2 expression was increased in both cell lines in response to adipose-conditioned media, but this increase was greater in the OE33R cells compared to the OE33P cells at 72 h ($p < 0.01$) (Fig. 3a). There was no difference in MAD2L2 expression between untreated OE33P and OE33R (data not shown). Levels of MAD2L2 expression in OE33R cells following 24 h treatment with adipose-conditioned media correlated with obesity status as measured by waist circumference ($R = 0.649$, $p = 0.05$) (Fig. 3b).

Adipose-conditioned media upregulates BUB1b expression

There was a fivefold increase in BUB1b expression in OE33P cells following 24 h of treatment with adipose-conditioned media ($p < 0.001$). In contrast there was a twofold

decrease in BUB1b expression following 72 h of adipose-conditioned media exposure ($p < 0.001$) (Fig. 4a). BUB1b expression was upregulated sixfold in OE33R cells treated with adipose-conditioned media for 24 h ($p < 0.01$), but downregulated fivefold in cells treated for 72 h ($p < 0.001$) (Fig. 4b). Following 72 h of adipose-conditioned media exposure, OE33R cells demonstrated significantly lower levels of BUB1b expression compared to OE33P cells ($p < 0.01$) (Fig. 4a). There was no difference in BUB1b expression between untreated OE33P and OE33R cells (data not shown). There was no difference in BUB1b expression following treatment with adipose-conditioned media from nonobese compared to obese patients (data not shown). BUB1b expression in OE33R cells at 24 h correlated with obesity status as measured by BMI ($R = 0.733$, $p = 0.04$) and waist circumference ($R = 0.716$, $p < 0.03$) (Fig. 4b, c).

Obese oesophageal adenocarcinoma patients demonstrate higher expression of MAD2L2 compared to nonobese patients

Expression of MAD2L2 and BUB1b in oesophageal adenocarcinoma tumour tissue samples from nonobese and obese patients was assessed using quantitative real-time PCR. Anthropometric data for oesophageal adenocarcinoma patients is summarised in Table 2 (supplementary

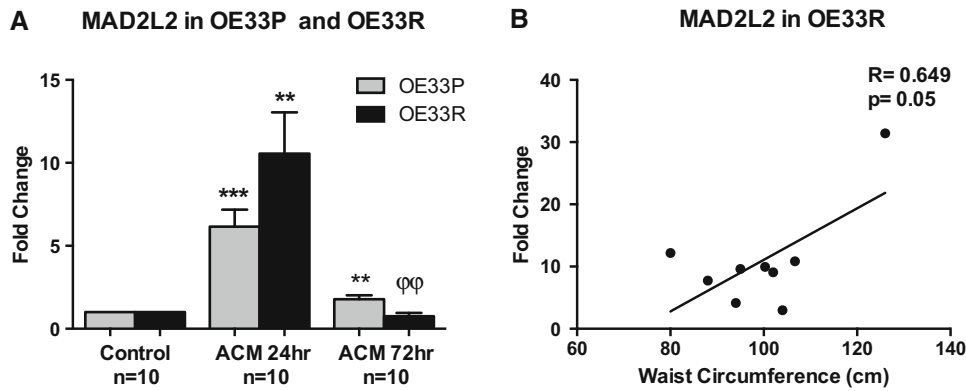


Fig. 3 OE33P and OE33R cell lines were treated with control media and adipose-conditioned media (ACM) for 24 and 72 h. Quantitative real-time PCR was carried out using a specific primer probe for MAD2L2. **a** Upregulation of MAD2L2 expression was detected in OE33P following ACM treatment for 24 ($p < 0.0001$) and 72 h ($p < 0.001$). ACM stimulated a tenfold upregulation of MAD2L2 expression in OE33R at 24 h ($p < 0.001$), but did not alter expression at 72 h. MAD2L2 expression was not significantly different in ACM-treated OE33P compared to ACM-treated OE33R at 24 h, but expression was higher in ACM-treated OE33P cells at 72 h ($p < 0.001$). Data are expressed as mean fold change in

expression \pm SEM for $n = 10$ patients, results represent the average from three independent experiments. Analysis was performed using paired Student’s *t* test to compare ACM-treated OE33P and OE33R versus controls, * $p < 0.05$, ** $p < 0.001$, *** $p < 0.0001$; an unpaired two-tailed Student’s *t* test was used to compare ACM-treated OE33P cells versus ACM-treated OE33R cells, $^{\phi}p < 0.05$, $^{\phi\phi}p < 0.001$, $^{\phi\phi\phi}p < 0.0001$. **b** MAD2L2 expression in OE33R at 24 h correlated with obesity status as measured by waist circumference ($R = 0.649$, $p = 0.05$). Analysis was performed using Pearson correlation coefficient. ACM adipose-conditioned media, *R* Pearson’s correlation coefficient

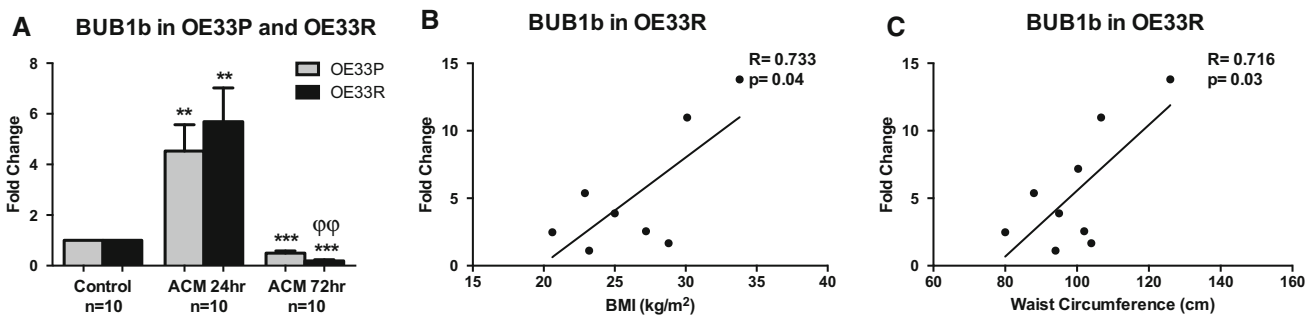


Fig. 4 OE33P and OE33R cell lines were treated with control media and adipose-conditioned media (ACM) for 24 and 72 h. Quantitative real-time PCR was carried out using a specific primer probe for BUB1B. **a** ACM upregulated BUB1b expression fivefold in OE33P at 24 h, and twofold in OE33P at 72 h. ACM upregulated BUB1b expression sixfold in OE33R at 24 h post-ACM treatment, and fivefold following 72 h of ACM treatment. There was no difference in BUB1b expression in ACM-treated OE33P cells compared to ACM-treated OE33R cells at 24 h, but BUB1b expression was significantly lower in OE33P compared to OE33R cells following 72 h of treatment. Data are expressed as mean fold change in expression \pm SEM for $n = 10$ patients, results represent the average from

three independent experiments. Analysis was performed using paired Student’s *t* test to compare ACM-treated OE33P and OE33R versus controls, * $p < 0.05$, ** $p < 0.001$, *** $p < 0.0001$; an unpaired two-tailed Student’s *t* test was used to compare ACM-treated OE33P cells versus ACM-treated OE33R cells, $^{\phi}p < 0.05$, $^{\phi\phi}p < 0.001$, $^{\phi\phi\phi}p < 0.0001$. BUB1b expression in OE33R at 24 h correlated with obesity status as measured by **b** BMI ($R = 0.733$, $p = 0.04$), and **c** waist circumference ($R = 0.716$, $p = 0.03$). Analysis was performed using Pearson correlation coefficient. ACM adipose-conditioned media, *R* Pearson’s correlation coefficient, *BMI* body mass index

data). Oesophageal adenocarcinoma tumour samples from visceraally obese patients ($n = 46$) demonstrated significantly higher levels of MAD2L2 expression compared to tumour samples from nonobese patients ($n = 41$, $p < 0.05$, Fig. 5a). There was no difference in BUB1b expression between tumour tissue from obese ($n = 46$) and nonobese patients ($n = 41$, $p = 0.5$, Fig. 5b).

Discussion

This study demonstrates that adipose tissue stimulates the genomic instability events anaphase bridge formation and spindle assembly complex dysregulation: visceraally obese oesophageal adenocarcinoma patients demonstrate higher MAD2L2 expression compared to nonobese patients.

Table 2 Anthropometric details for viscerally obese and nonobese oesophageal adenocarcinoma patients selected for validation of spindle assembly checkpoint gene expression

	Nonobese (<i>n</i> = 46)	Obese (<i>n</i> = 41)	<i>p</i> value
Age at surgery (years)*	65 (42–86)	64 (45–83)	NS ^a
Gender			
Male/female	35/11	33/8	NS ^b
Obesity status			
Body mass index (kg/m ²)*	23.4 (10.1–33.6)	29.3 (18.3–39)	<0.0001 ^a
Waist circumference (cm)*	88 (61–109)	101 (85–130)	<0.0001 ^a
Visceral fat area (cm ²)*	73.9 (4.3–158)	211.4 (110.6–381.1)	<0.0001 ^a
Neoadjuvant therapy			
Yes/no	23/23	21/18	NS ^b
Pathological <i>T</i> stage			NS ^c
Tis	0	1	
T0	5	19	
T1	6	0	
T2	6	7	
T3	29	12	
T4	0	1	
Tx	0	1	

The two cohorts were equivalent except for statistically significant differences in markers of obesity (body mass index, waist circumference, visceral fat area)

Statistical analysis was performed using Mann–Whitney *U* test for *n* = 87 patients

* *p* < 0.05, ** *p* < 0.001, *** *p* < 0.0001, NS nonsignificant

* Values given are median (range); NS not significant

^a Analysis performed using Mann–Whitney *U* test

^b Analysis performed using Fisher's exact test

^c Pathological *T* stage 0–2 compared to pathological *T* stage 3–4, analysis performed using Fisher's exact test

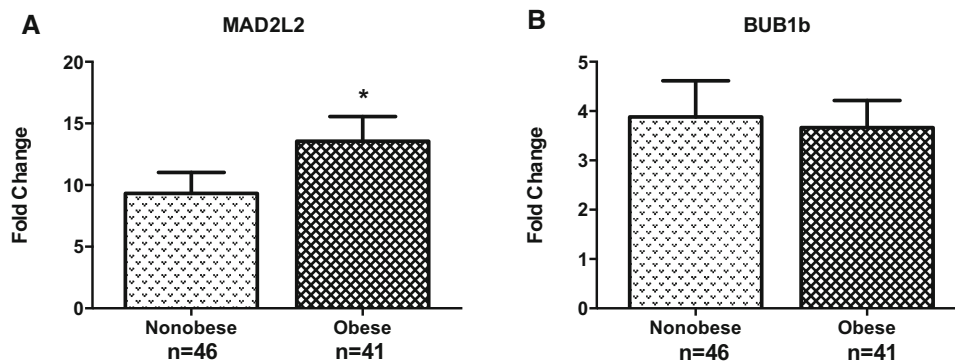


Fig. 5 MAD2L2 and BUB1B expression levels were determined in oesophageal adenocarcinoma tumour samples from nonobese and obese patients using quantitative real-time PCR. **a** Tumour samples from obese patients demonstrated significantly higher levels of MAD2L2 expression compared to tumour samples from nonobese

patients (*p* < 0.05). **b** There was no difference in BUB1B expression in tumour samples from nonobese patients compared to tumour samples from obese patients. Data are expressed as median relative quantification (RQ) values ± SEM. Statistical analysis was performed using Mann–Whitney *U* test, **p* ≤ 0.05

Furthermore, anaphase bridge levels are higher in radioresistant compared to radioresponsive oesophageal cancer cells.

This is the first study to demonstrate that visceral adipose tissue stimulates anaphase bridge formation in

oesophageal adenocarcinoma. Anaphase bridges are a functional, mechanistic marker of genomic instability. The breakage–fusion–bridge cycle links telomere shortening and anaphase bridge formation. The question of which exposures or lifestyle factors drive anaphase bridge

formation has not previously been addressed in the literature, but telomere shortening in leucocytes has been linked to obesity and obesity-related conditions such as diabetes mellitus [11]. Telomere shortening in Barrett's oesophagus is inversely correlated with subsequent risk of adenocarcinoma [6]. Our study further highlights the link between obesity and genomic instability in oesophageal adenocarcinoma.

Anaphase bridge formation correlated with obesity status as measured by body mass index, waist circumference and, importantly, visceral fat area. Visceral fat area is the gold standard marker of obesity and visceral fat is more metabolically active than subcutaneous fat, therefore one would expect the downstream effects of obesity to correlate with visceral rather than overall adiposity [17].

Live cell imaging showed that the majority of anaphase bridges formed will break, usually unevenly, giving rise to structural chromosomal rearrangement [22]. In this study, adipose-conditioned media induced anaphase bridge formation in both OE33P and OE33R cells, but bridging was significantly higher in OE33R. Anaphase bridge formation was maximal at 24 h, in keeping with previous reports that levels of bridges decrease by 72 h in accordance with preferential breakage fate of bridges during cell division [22].

This is the first study demonstrating that increased levels of anaphase bridge formation are associated with radioresistance, and that levels of anaphase bridges correlate with obesity status in radioresistant cells. Genomic instability is associated with intrinsic taxane resistance in ovarian cancer and multi-drug resistance in colorectal cancer [9, 10]. Telomere dysfunction has been associated with altered radiosensitivity [23, 24]. Telomerase-deficient *Terc*^{-/-} mice that also demonstrated telomere shortening and increased anaphase bridge formation exhibited a radiosensitive phenotype associated with accelerated mortality [23]. Anaphase bridge formation is easily measured in vitro. Due to the heterogenous cell population typical of tumour samples, and low proportion of cells in this transient configuration, anaphase bridge quantification in patient samples is much more difficult. Thus anaphase bridge measurement has limited usefulness as a biomarker of radiosensitivity in vivo [5].

Our group has demonstrated that the radioresistance of the OE33R cells is due at least in part to alterations in DNA damage repair efficiency [18]. Anaphase bridges are associated with DNA double strand breaks (DSBs) [25]. While the majority of DSBs are repaired correctly, restoring the original chromosome structure, misalignment of two non-matching ends may also occur resulting in anaphase bridges and chromosomal instability [25]. Non-homologous end joining (NHEJ) acts to prevent anaphase bridges and in its absence the activity of homologous

recombination (HR) leads to anaphase bridge formation; intrinsic NHEJ activity correlates with the induction of anaphase bridges, suggesting a mechanistic link between genomic instability and radioresistance [25].

Visceral fat area is an independent predictor of outcome after anti-angiogenic treatment in colorectal and renal cell cancer, indicating that angiogenic factors produced by visceral fat may influence tumour progression and response to chemotherapy [12, 13]. Increasing BMI is associated with a higher rate of recurrence following adjuvant chemoradiotherapy in rectal cancer and treatment failure following radiotherapy in prostate cancer [26, 27]. Visceral adipose-conditioned media in oesophageal adenocarcinoma patients is a rich source of adiponectin, leptin and numerous cytokines such as TNF- α , IL-6, monocyte chemoattractant protein-1 (MCP-1), IL-8, IL-10 and VEGF. These factors have been implicated in tumour progression. Treatment of oesophageal cancer cells with recombinant IL-6 and VEGF results in dose-dependent increases in cellular proliferation, while neutralising VEGF significantly reduces cellular proliferation [17]. VEGF is a pro-angiogenic and survival factor for a variety of solid malignancies. Recent studies highlighted a role for anti-VEGF therapies prior to radiotherapy in a variety of tumour model systems including oesophageal adenocarcinoma [28]. VEGF is currently under investigation as a therapeutic target for radiosensitisation in rectal cancer [29]. We speculate that some of the biologically active factors in visceral adipose tissue drive genomic instability events in radioresistant oesophageal cancer cells, implying that adipokines influence cancer behaviour and response to therapy.

Adipose-conditioned media upregulates expression of MAD2L2 and BUB1b in radioresponsive and radioresistant oesophageal adenocarcinoma in vitro. Obese oesophageal cancer patients demonstrate increased expression of MAD2L2 but not BUB1b in their tumour specimens. The reason for the discordant BUB1B expression in in vitro and in vivo data is unclear. BUB1b overexpression may be a tumour-specific effect, and the heterogenous cell population typical of tumour samples may mask the effect of obesity on tumour epithelial cells. Obesity has not previously been linked with spindle assembly complex disruption. Studies identifying causal mechanisms for spindle assembly complex deregulation are lacking, although oxidative stress has been linked to malfunction of the spindle assembly complex in yeast [30]. Alterations in MAD2L2 expression drive tumorigenesis in mice and are seen in number of human epithelial cancers [31, 32]. BUB1b has a number of roles in the spindle assembly complex and overexpression of this gene has been reported in colorectal cancer [33]. Doak et al. reported both under and over expression of both MAD2L2 and BUB1b genes in

Barrett's oesophagus specimens, but spindle assembly complex disruption has not previously been documented in oesophageal adenocarcinoma [34].

Anaphase bridge formation did not correlate with alterations in BUB1b or MAD2L2 expression. Prencipe et al. demonstrated that deregulation of MAD2L2 was associated with increased anaphase bridge formation and polyploidy in breast cancer cell lines [32]. Spindle assembly complex deregulation is linked to genomic instability in a number of cancer types, but genomic instability may still occur in the presence of an intact spindle assembly complex, suggesting that while both anaphase bridge formation and a compromised spindle assembly complex are conducive to aneuploidy and carcinogenesis, these processes may occur independently of each other [32, 33]. A weakened spindle assembly complex may function as a facilitator rather than a driving force of tumorigenesis.

This study demonstrates a novel role for visceral obesity in the induction of genomic instability events and highlights the complex interaction between obesity, genomic instability and radioresponse in oesophageal adenocarcinoma. Identification of the factors driving anaphase bridge formation could identify shared pathways as potential preventative and therapeutic targets, enabling the stratification of patients based on predicted response to therapy and ultimately to the manipulation of these factors to sensitise resistant cells to radiation.

Acknowledgments We would like to thank the members of the oesophageal surgical team at St. James's hospital. We would also like to thank all the patients who gave their consent for sample procurement. This work was supported by funding from the Health Research Board (HPF/2011/59).

Compliance with ethical standards

Conflict of interest The authors declare that they have no conflicts of interest.

References

- Doyle SL, Donohoe CL, Lysaght J, Reynolds JV. Visceral obesity, metabolic syndrome, insulin resistance and cancer. *Proc Nutr Soc*. 2012;71:181–9.
- Calle EE, Rodriguez C, Walker-Thurmond K, Thun MJ. Overweight, obesity, and mortality from cancer in a prospectively studied cohort of US adults. *New Engl J Med*. 2003;348:1625–38.
- Negrini S, Gorgoulis VG, Halazonetis TD. Genomic instability—an evolving hallmark of cancer. *Nat Rev Mol Cell Biol*. 2010;11:220–8.
- Sampson MJ, Winterbone MS, Hughes JC, Dozio N, Hughes DA. Monocyte telomere shortening and oxidative DNA damage in type 2 diabetes. *Diabetes Care*. 2006;29:283–9.
- O'Sullivan JN, Bronner MP, Brentnall TA, Finley JC, Shen WT, Emerson S, et al. Chromosomal instability in ulcerative colitis is related to telomere shortening. *Nat Genet*. 2002;32:280–4.
- Finley JC, Reid BJ, Odze RD, Sanchez CA, Galipeau P, Li S, et al. Chromosomal instability in Barrett's esophagus is related to telomere shortening. *Cancer Epidemiol Biomarkers Prev*. 2006;15:1451–7.
- McClintock B. The stability of broken ends of chromosomes in *Zea mays*. *Genetics*. 1941;26:234–82.
- Li M, Zhang P. Spindle assembly checkpoint, aneuploidy and tumorigenesis. *Cell Cycle*. 2009;8:3440.
- Lee AJ, Endesfelder D, Rowan AJ, Walther A, Birkbak NJ, Futreal PA, et al. Chromosomal instability confers intrinsic multidrug resistance. *Cancer Res*. 2011;71:1858–70.
- Swanton C, Nicke B, Schuett M, Eklund AD, Ng C, Li Q, et al. Chromosomal instability determines taxane response. *Proc Natl Acad Sci USA*. 2009;106:8671–6.
- Sampson MJ, Winterbone MS, Hughes JC, Dozio N, Hughes DA. Monocyte telomere shortening and oxidative DNA damage in type 2 diabetes. *Diabetes Care*. 2006;29:283–9.
- Ladoire S, Bonnetain F, Gauthier M, Zanetta S, Petit JM, Guiu S, et al. Visceral fat area as a new independent predictive factor of survival in patients with metastatic renal cell carcinoma treated with antiangiogenic agents. *Oncologist*. 2011;16:71–81.
- Guiu B, Petit JM, Bonnetain F, Ladoire S, Guiu S, Cercueil JP, et al. Visceral fat area is an independent predictive biomarker of outcome after first-line bevacizumab-based treatment in metastatic colorectal cancer. *Gut*. 2010;59:341–7.
- Ronellenfötsch U, Schwarzbach M, Hofheinz R, Kienle P, Kieser M, Slinger TE, Jensen K, et al. Perioperative chemo(radio)therapy versus primary surgery for resectable adenocarcinoma of the stomach, gastroesophageal junction, and lower esophagus. *Cochrane Database Syst. Rev*. 2013;5:CD008107.
- Sjoquist KM, Burmeister BH, Smithers BM, Zalcberg JR, Simes RJ, Barbour A, et al. Survival after neoadjuvant chemotherapy or chemoradiotherapy for resectable oesophageal carcinoma: an updated meta-analysis. *Lancet Oncol*. 2011;12:681–92.
- Van Hagen P, Hulshof MC, van Lanschot JJ, Steyerberg EW, van Berge Henegouwen MI, Wijnhoven BP, et al. Preoperative chemoradiotherapy for esophageal or junctional cancer. *N Engl J Med*. 2012;366:2074–84.
- Lysaght J, van der Stok EP, Allott EH, Casey R, Donohoe CL, Howard JM, et al. Pro-inflammatory and tumour proliferative properties of excess visceral adipose tissue. *Cancer Lett*. 2011;312:62–72.
- Lynam-Lennon N, Reynolds JV, Pidgeon GP, Lysaght J, Marignol L, Maher SG. Alterations in DNA repair efficiency are involved in the radioresistance of esophageal adenocarcinoma. *Radiat Res*. 2010;174:703–11.
- Doyle SL, Bennett AM, Donohoe CL, Mongan AM, Howard JM, Lithander FE, et al. Establishing computed tomography-defined visceral fat area thresholds for use in obesity-related cancer research. *Nutr Res*. 2013;33:171–9.
- Ibrahim NB. ACP. Best practice no 155. Guidelines for handling oesophageal biopsies and resection specimens and their reporting. *J Clin Pathol*. 2000;53:89–94.
- Fried SK, Moustaid-Moussa N. Culture of adipose tissue and isolated adipocytes. *Methods Mol Biol*. 2001;155:197–212.
- Pampalona J, Frias C, Genesca A, Tusell L. Progressive telomere dysfunction causes cytokinesis failure and leads to the accumulation of polyploid cells. *PLoS Genet*. 2012;8:e1002679.
- Wong KK, Chang S, Weiler SR, Ganesan S, Chaudhuri J, Zhu C, et al. Telomere dysfunction impairs DNA repair and enhances sensitivity to ionizing radiation. *Nat Genet*. 2000;26:85–8.
- McCaul JA, Gordon KE, Minty F, Fleming J, Parkinson EK. Telomere dysfunction is related to the intrinsic radio-resistance of human oral cancer cells. *Oral Oncol*. 2008;44:261–9.
- Acilan C, Potter DM, Saunders WS. DNA repair pathways involved in anaphase bridge formation. *Genes Chromosomes Cancer*. 2007;46:522–31.
- Meyerhardt JA, Tepper JE, Niedzwiecki D, Hollis DR, McCollum AD, Brady D, et al. Impact of body mass index on outcomes and treatment-related toxicity in patients with stage II and III rectal cancer: findings from Intergroup Trial 0114. *J Clin Oncol*. 2004;22:648–57.
- Efstathiou JA, Chen M-HH, Renshaw AA, Loffredo MJ, D'Amico AV. Influence of body mass index on prostate-specific antigen failure after androgen suppression and radiation therapy for localized prostate cancer. *Cancer*. 2007;109:1493–8.
- Wachsberger P, Burd R, Dicker AP. Tumor response to ionizing radiation combined with antiangiogenesis or vascular targeting agents: exploring mechanisms of interaction tumor response to ionizing radiation combined with antiangiogenesis or vascular targeting agents: exploring mechanisms. *Clin Cancer Res*. 2003;9:1957–71.
- Willett CG, Boucher Y, di Tomaso E, Duda DG, Munn LL, Tong RT, et al. Direct evidence that the VEGF-specific antibody bevacizumab has antivascular effects in human rectal cancer. *Nat Med*. 2004;10:145–7.
- D'Angiolella V, Santarpia C, Grieco D. Oxidative stress overrides the spindle checkpoint. *Cell Cycle*. 2007;6:576–9.
- Sotillo R, Hernando E, Diaz-Rodriguez E, Teruya-Feldstein J, Cordon-Cardo C, Lowe SW, et al. Mad2 overexpression promotes aneuploidy and tumorigenesis in mice. *Cancer Cell*. 2007;11:9–23.
- Prencipe M, Fitzpatrick P, Gorman S, Tosetto M, Klinger R, Furlong F, et al. Cellular senescence induced by aberrant MAD2 levels impacts on paclitaxel responsiveness in vitro. *Br J Cancer*. 2009;101:1900–8.
- Cahill DP, Lengauer C, Yu J, Riggins GJ, Willson JK, Markowitz SD, et al. Mutations of mitotic checkpoint genes in human cancers. *Nature*. 1998;392:300–3.
- Doak SH, Jenkins GJ, Parry EM, Griffiths AP, Baxter JN, Parry JM. Differential expression of the MAD2, BUB1 and HSP27 genes in Barrett's oesophagus—their association with aneuploidy and neoplastic progression. *Mutat Res*. 2004;547:133–44.